4-3-2019

Application of the CLAYFF and the DREIDING force fields for modeling of alkylated quartz surfaces

Aleksandr Abramov
Edith Cowan University

Stefan Iglauer
Edith Cowan University

10.1021/acs.langmuir.9b00527

Application of the CLAYFF and the DREIDING Force Fields for Modelling of Alkylated Quartz Surfaces

Aleksandr Abramov*, Stefan Iglauer, School of Engineering, Edith Cowan University, 270 Joondalup Drive, Joondalup, WA 6027, Western Australia, Australia

*aabramov@our.ecu.edu.au

Abstract

To extend applicability and to overcome limitations of combining rules for non-bond potential parameters, in this study CLAYFF and DREIDING force fields are coupled at the level of atomic site charges to model quartz surfaces with chemisorpt hydrocarbons. Density functional theory and Bader charge analysis are applied to calculate charges of atoms of the OC bond connecting quartz crystal and an alkyl group. The study demonstrates that the hydrogen atom of the quartz surface hydroxyl group can be removed and its charge can be redistributed among the oxygen and carbon atoms of the OC bond in a manner consistent with results calculated at the density functional level of theory. Augmented with modified charges of the OC bond, force fields can then be applied to a practical problem of evaluation of the contact angle of a water droplet on alkylated quartz surfaces in a carbon dioxide environment, which is relevant for carbon geo-sequestration and in a broader context of oil and gas recovery. Alkylated quartz surfaces have been shown to be extremely hydrophobic even when the surface density of hydroxyl groups is close to the highest naturally observed density of 6.2 OH groups per square nanometre.

Key words: molecular dynamics, force fields, alkylated quartz, wettability, carbon dioxide

Introduction

In realistic implementations of carbon capture and storage technology, coal beds and depleted oil or gas reservoirs are considered possible storage mediums [1-2]. Within these formations mineral surfaces aged in oil, alkylated surfaces with chemisorpt hydrocarbons, and composed of organic matter coal are interfaces encountered by stored CO_2. Experimental studies indicate that in these structures surfaces of minerals are in the best case intermediate wet and can be strongly CO_2-wet [3-4]. Recent experiments have shown that even minute concentrations of organics adsorbed on crystal surfaces can change their wetting behaviour [5]. To understand the wetting of minerals in CO_2 atmosphere at the atomistic level, molecular dynamics and force fields are widely used [6-18]. Some force fields are specifically designed to reproduce properties of crystals and minerals, like the BKS (van Beest, Kramer, van Santen) potential [19], the INTERFACE force field [20] or the CLAYFF force field [21]. Others are well suited to reproduce properties of organic molecules or hydrocarbons, for example the MM3 [22], the MM4 [23] and the DREIDING [24] force fields. However, it is not always possible to couple these force fields using the combining rules for parameters of non-bond potentials only, e.g. the Lorentz-Berthelot rules [25-26]. The most obvious case where this coupling is not straightforward is when organic molecules are chemisorpt on the mineral surface. When the mineral is quartz, the second most abundant mineral in the Earth's continental crust [27-28], the formation of the OC bond linking the crystal and the organic molecule creates a problem. Charges on both atomic sites of the bond may not be supplied by either of the force fields or may not correspond to the required chemical environment.

In computational chemistry in general and classical molecular dynamics in particular, charge is the first order parameter that affects and defines interactions between atomic sites. Electrostatic interactions are long range [29] and have significant impact on calculated properties and molecular geometries. Further to this, partial charges are sometimes derived to reproduce known thermodynamic data [30-32]. Therefore, it follows that assignment of correct partial charges to atomic sites is of primary importance for obtaining physically meaningful results from molecular dynamics simulations.

In this work the researchers utilize the predictive capabilities of DREIDING and CLAYFF force fields in realms of organic molecules and minerals, respectively, and further enhance the domain of their applicability by augmenting them with charges on atomic sites of the polar OC bond connecting the quartz crystal to an alkyl group. Modified using density functional theory, force fields are then applied to predicting the contact angle of a water droplet on alkylated quartz surfaces in carbon dioxide atmosphere. These force fields have been selected because of their versatility in their corresponding areas, covered range of organic molecules and minerals, and because of their compatibility in the approach in handling electrostatics (interactions between partial charges versus interactions between dipoles of polar bonds).

Computational Methodology

A variety of computational methods ranging from approaches to compute the electronic structure of periodic systems to classical molecular dynamics have been applied in this research. Density Functional Theory (DFT) calculations were performed with version 6.3 of the Quantum ESPRESSO suite of computer codes. From the suite the PWscf and PostProc programs [33-34] were used. The Bader charge analysis [35] was performed with version 1.03 of "Code: Bader Charge Analysis" [36-39]. The DL_POLY 4.08 package for general purpose parallel molecular dynamics simulations was applied to perform classical molecular mechanics computations [40-41]. The DL_POLY Graphical User Interface was used to prepare a model of C_5H_{11} group. Visualizations of the simulation results were created with VMD [42] and VESTA [43] software. The VESTA program was also used for manipulations with periodic and molecular structures.

In all classical molecular dynamics simulations the velocity Verlet algorithm [44] was used to integrate the equations of motion. The time step in all simulations was set to 2 fs. The Nose-Hoover thermostat and barostat [45-46] with the relaxation constants 0.05 and 0.5 ps, respectively, were used in the NPT simulations. The Nose-Hoover thermostat with the relaxation constant 0.05 ps was used in the NVT simulations. Electrostatic interactions were calculated using the smoothed particle mesh Ewald summation [47-48]. Distance for the interactions cutoff was fixed to 17 A in all simulations. The force field for molecular dynamics simulations was constructed as a combination of several potential models. Quartz crystal, the hydroxylated quartz surface and the Simple Point-Charge (SPC) water [49] were modelled with parameters of the CLAYFF force field [21]. Carbon dioxide was represented by the Elementary Physical Model (EPM2) [50]. Chemisorpt pentyl groups were simulated with the DREIDING force field [24]. Transferable ab-initio DFT calculations, where the constraints on the exchange-correlation hole are used to derive the energy functional [51], were used to rationalize parameters applied for coupling the CLAYFF and the DREIDING force fields, specifically the charges on atoms of the OC bond connecting alkyl groups to quartz. Detailed specifications of used force fields and computational parameters are provided in the Supporting Information.

Results and Discussion

Coupling of the CLAYFF and the DREIDING Force Fields

We consider the fully hydroxylated quartz surface [52-54] as the starting point to construct alkylated systems. The surface is described in a consistent way by the CLAYFF force field with all atomic species having certain charges and at the same time providing overall charge neutrality. To model an alkylated quartz surface we populate it with pentyl groups which are described by the DREIDING force field where all atomic species are neutral. To integrate a pentyl group on top of the surface a hydrogen atom of the silanol group has to be removed to create the OC bond where the oxygen atom belongs to the surface and the carbon atom belongs to the pentyl rest, see Figure 1. Note that one hydrogen atom of the pentane molecule has to be removed, to form the C_5H_{11} group. These manipulations create alkylated quartz surfaces with chemisorpt pentyl groups and frustrate overall charge neutrality.

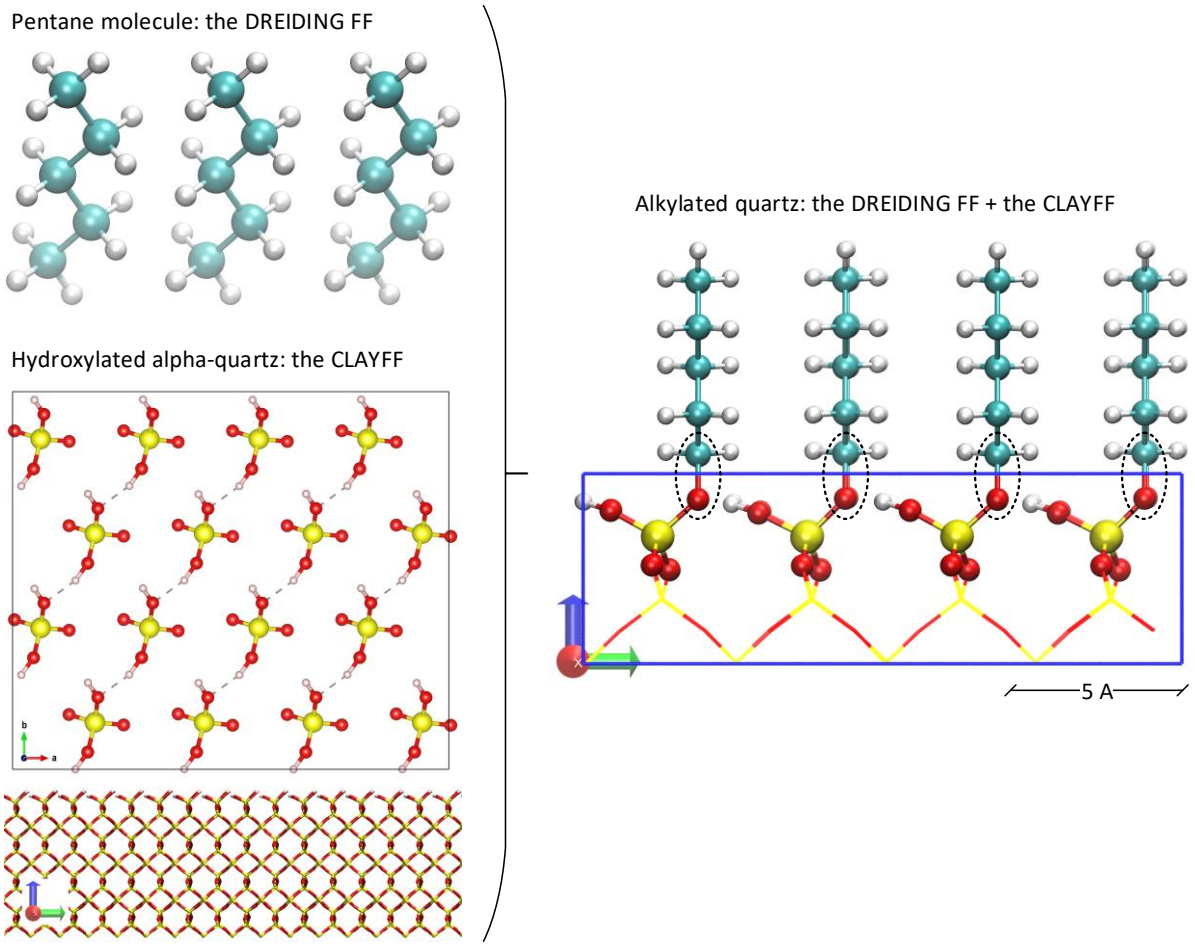

Figure 1. Conceptual illustration of the force fields coupling problem. White balls - hydrogen atoms, red balls - oxygen atoms, light blue balls - carbon atoms, yellow balls - silicon atoms. Top and side views of the quartz surface/crystal are shown on the left, a side view of the alkylated quartz is shown on the right. The polar OC bond is highlighted with dashed ellipses. FF stands for Force Field.

The charge neutrality is violated by the removal of the hydrogen atom from a silanol group which in the CLAYFF force field has a positive charge of 0.425 e. Accompanying this modification, the creation of a polar OC bond should compensate for the charge imbalance. To make physically meaningful corrections to combined CLAYFF and DREIDING force fields we use DFT to calculate how much of the removed positive charge should be assigned to the carbon atom and how much of it should remain with the oxygen atom of the OC bond.

Modelling of the OC bond is performed within a sufficiently large but scaled down system studied here with classical molecular dynamics. This representative model is built as follows. Out of the orthorhombic quartz crystal cell [55] a super cell 2x1x1 is constructed (overall 36 atoms, 12 silicon atoms and 24 oxygen atoms). Using this supercell the following DFT calculations are then executed in three stages. In the first stage the lattice vectors of the crystal are allowed to be changed and optimized during accurate relaxation of ionic positions of the cell. In the second stage a three-layer slab is constructed with fully hydroxylated surface and integrated pentyl group, 30 A of vacuum space is provided above the surface, see Figure S1 in the Supporting Information. Only ions of this system are then relaxed using less demanding computational parameters (see the next paragraph for details) with atoms of the bottom layer (one height of the primitive unit cell) of the slab being fixed. In the third stage the charge density distribution of the relaxed slab is determined with an accurate single point energy calculation.

This single point energy calculation results in the most important output for the purpose of this study, the distribution of the charge density. Thus, in the third and in the first (to get accurate lattice constants)

computational stages kinetic energy cutoffs for plane waves and for charge density were set to high values of 40 and 1500 Ry, respectively. In the second stage these parameters were set to 20 and 700 Ry, respectively. To sample the first Brillouin zones in reciprocal space we used Monkhorst-Pack meshes [56] 5x5x7, 3x3x1 and 5x5x1, for the first through the third stages of calculations, respectively. We used the projector augmented wave method (PAW) [57] potentials H.pbe-kjpaw_psl.0.1.UPF, C.pbe-n-kjpaw_psl.0.1.UPF, O.pbe-n-kjpaw_psl.0.1.UPF and Si.pbe-n-kjpaw_psl.0.1.UPF from [58]. In all DFT calculations the electron exchange and correlation energy was approximated by the Perdew-Burke-Ernzerhof functional [51].

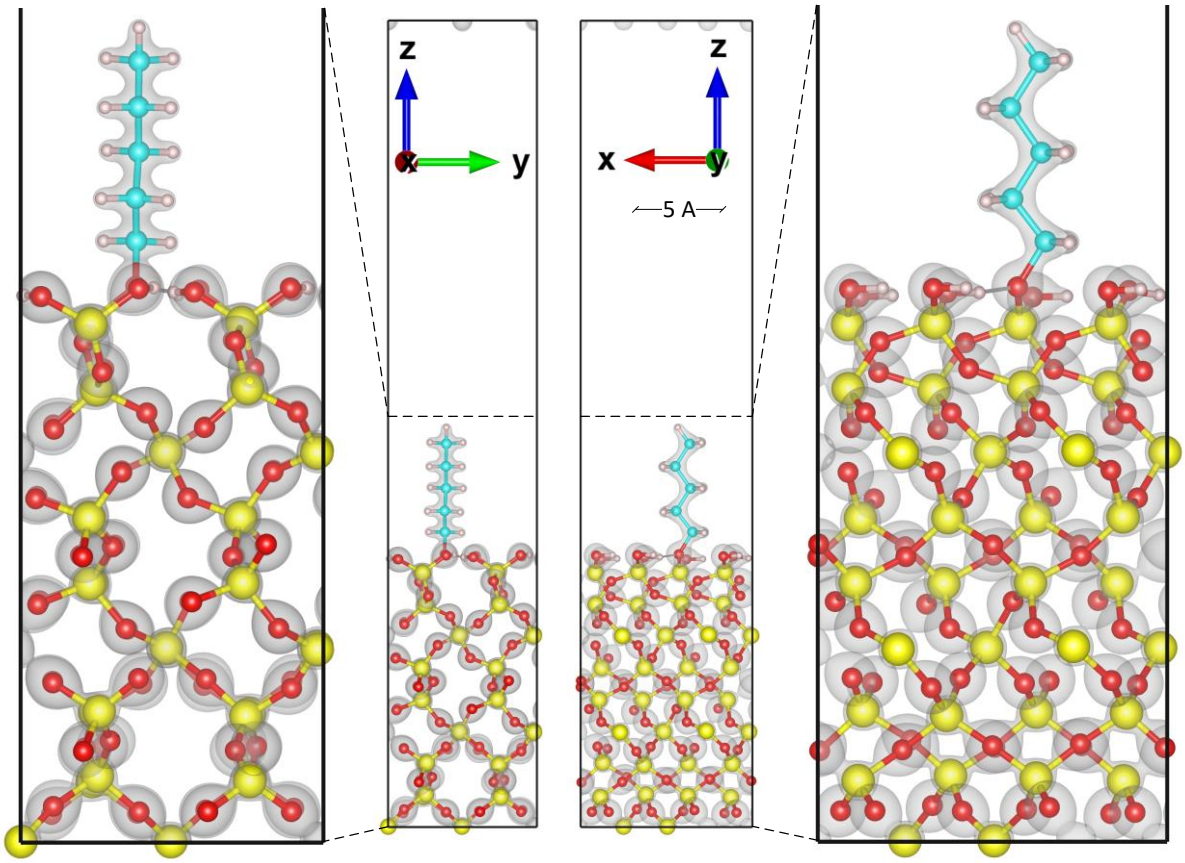

Figure 2. Charge density distribution of the three-layer quartz slab computed at the DFT level of theory, views along x (left) and y (right) axises. White balls - hydrogen atoms, light blue balls - carbon atoms, red balls - oxygen atoms, yellow balls - silicon atoms. Grey halo shows the iso-surface of the charge density, the iso-value was chosen such that the charge clouds around the oxygen and silicon atoms just start to overlap.

Computed lattice constants of the unit cell of the quartz crystal amounted to 9.8389x8.5175x5.4209 A. These lattice constants are in perfect agreement with the crystallographic lattice constants obtained from [59], they are only by 0.03 to 0.3% larger. The calculated charge density distribution of the model system is shown in Figure 2. Within the crystal, the electron charge density is predominantly localized around oxygen atoms. Hydroxyl oxygen atoms are the main attractors of electron density as well. The Bader analysis reveals a quantitative picture of charge distribution around the OC bond connecting the quartz crystal and the C_5H_{11} group, thus the charge of the oxygen atom is -1.311489 e, and charge of the carbon atom is 0.338301 e. This positive carbon charge corresponds to 0.796 of the charge on the hydroxyl hydrogen of the CLAYFF force field. We assign this fraction of the CLAYFF hydroxyl hydrogen charge to the carbon of the OC bond for two reasons. The first is that this figure is the only physically substantiated number which minimizes absolute charge difference between our modified force field and the DFT results for two atoms of the OC bond, see Figure 3. The second reason is that the rest of the hydroxyl hydrogen charge assigned to the oxygen of the OC bond renders the atom approximately 90% as negative (-0.863301 e) as the other hydroxyl oxygen of the geminal silanol group (-0.95 e) of the

CLAYFF force field. This 90% proportion agrees well with results of the Bader charge analysis where the charges on these two oxygen atoms of the same geminal silanol group are -1.311489 and -1.477656 e, respectively. With these operations we resolved two problems related to the coupling of the CLAYFF and the DREIDING force fields. We replaced the hydroxyl hydrogen with carbon of the pentyl group, and redistributed the charge of the replaced hydrogen atom between the carbon and the oxygen atoms of the OC bond in a manner consistent with the DFT results.

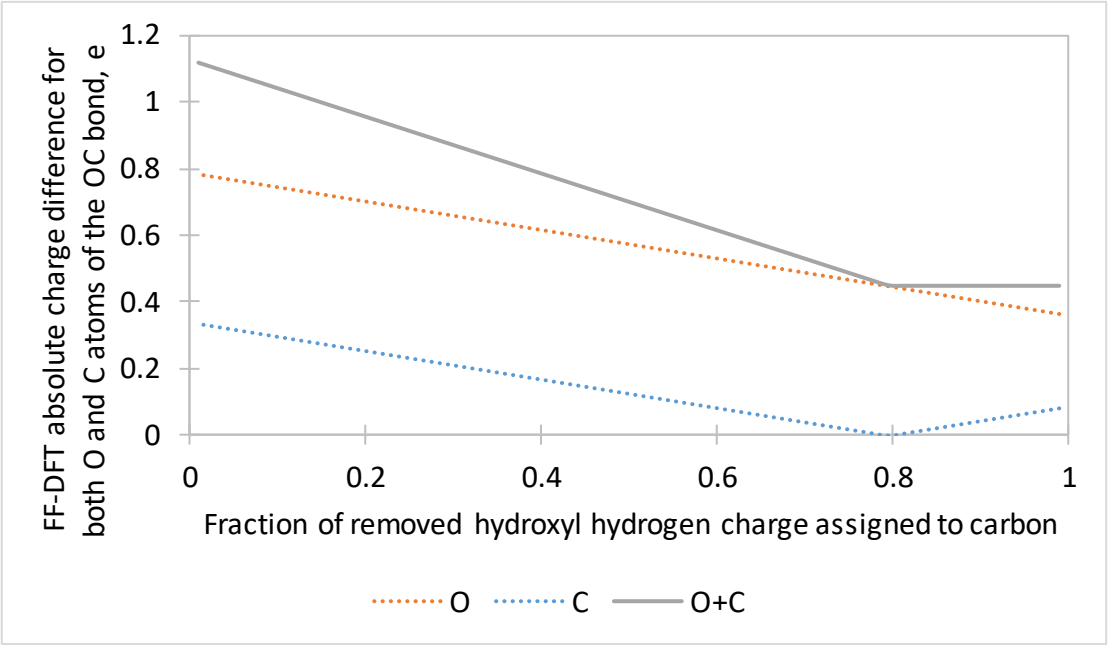

Figure 3. Absolute charge difference between modified force field and DFT results for the two atoms of the OC bond. FF stands for Force Field.

In addition, for comparison we report charges on some other atoms and geometrical characteristics of some bonds obtained at the DFT level of theory. Excluding carbon of the OC bond, the average charges on carbon and hydrogen atoms of the C_5H_{11} group were found to be -0.0298 and 0.0311 e, respectively. This is in alignment with the DREIDING force field where these charges are set to zero. Average CH and CC bond lengths of the C_5H_{11} group amounted to 1.1637 and 1.52998 A, respectively. OC and SiO bond lengths were calculated to be 1.5024 and 1.6689 A, respectively. The DREIDING force field demonstrates good agreement with these values as well, reproducing from 89 to 100% of the bond lengths.

Summing up the results of this DFT study we conclude that the obtained charge distribution for the OC bond connecting quartz crystal and the alkyl rest can be applied to investigate properties of quartz surfaces with chemisorpt hydrocarbons. The charge of the replaced hydroxyl hydrogen of the CLAYFF force field is distributed among the oxygen and carbon atoms of the created OC bond in proportion 0.204 to 0.796, which results in charges on the oxygen and the carbon atoms of -0.863301 and 0.338301 e, respectively. Such charge distribution stems from the electronic structure calculations, and couples the CLAYFF and the DREIDING force fields, thus preserving overall system neutrality without a need to introduce arbitrary ions.

Application of Modified Force Fields to Alkylated Quartz Surfaces

As an example of the application of coupled in described above manner the CLAYFF and DREIDING force fields, we examine two hydroxylated quartz surfaces with pentyl group concentrations 1.45 and 2.89 C_5H_{11}/nm^2, see Figure 4. The alkylated surfaces were constructed using fully hydroxylated (001) α-quartz surface previously reconstructed in [52-54]. Using the primitive unit cell of α-quartz [59] its orthorhombic cell was produced according to [55]. Out of this cell a large enough super cell was created

to equilibrate the quartz crystal at 1 atm pressure and 300 K temperature over 10^5 steps in the NPT ensemble. Obtained crystal structure and lattice constants were then used to create four-layer (four primitive unit cell heights) quartz slab which was relaxed at 10 K for 10^5 steps in the NVT ensemble to obtain the initial ordered surface structure. Atoms of the basal layer (one primitive unit cell height) of the slab were fixed to emulate the bulk crystal in all calculations (the slab and the fully assembled systems).

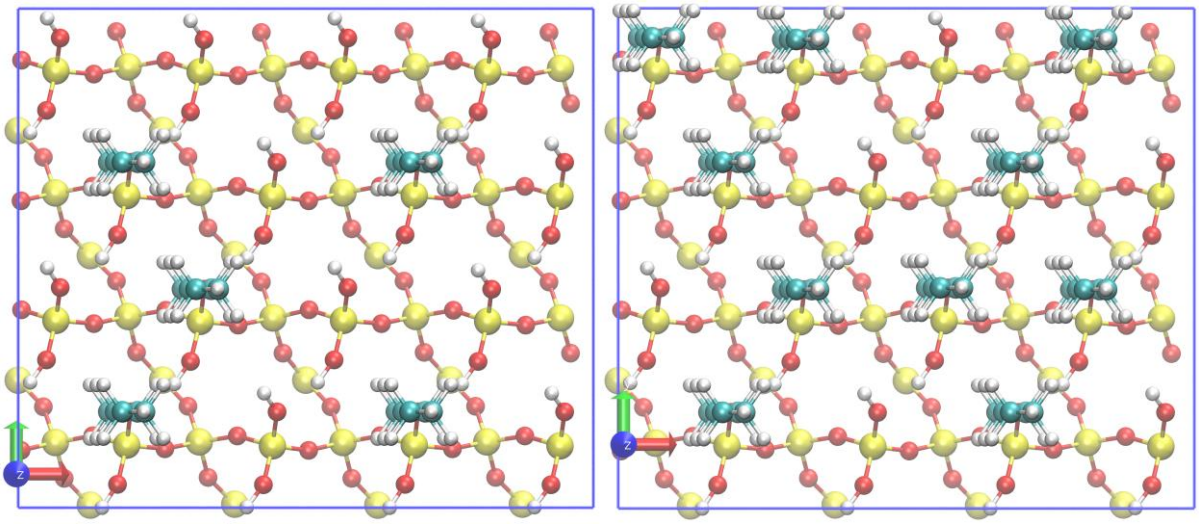

Figure 4. Top layers of the surface unit cells of hydroxylated quartz with a pentyl surface group concentration of 1.45 (left) and 2.89 C_5H_{11}/nm^2 (right). White balls - hydrogen atoms, light blue balls - carbon atoms, red balls - oxygen atoms, yellow balls - silicon atoms.

Two models containing a water droplet, CO_2 gas and quartz with integrated surface pentyl groups were prepared next. Simulations were performed at 300 K and 10 MPa of CO_2 pressure. The number of CO_2 molecules corresponding to this PT-conditions for every model was determined according to [60] and amounted to 6984 and 6677 for surfaces with a C_5H_{11} density of 1.45 and 2.89 pentyl groups per square nanometre, respectively. Water density 1000 kg/m^3 was used. Uniformly distributed carbon dioxide and water molecules were pre-equilibrated at 300 K in 100x104x60 and in 50x50x50 A boxes, respectively. Dynamics of these two systems were modelled in the NVT ensembles, with 5×10^5 steps performed for CO_2 and 10^5 steps for H_2O. Then, a half sphere of radius 26 A atop of C_5H_{11} groups was filled with water molecules from the above described pre-equilibration box. 946 H_2O molecules fit into the "water droplets", which were placed in the centre of the slabs. The rest of the space up to 60 A above C_5H_{11} groups was filled with pre-equilibrated carbon dioxide. Vacuum space of 70 A was provided on top of 60 A above the C_5H_{11} groups. All simulations were performed with periodic boundary conditions in x and y directions, and in z direction a repulsive force was applied at 60 A above the tip level of C_5H_{11} groups:

$$F = k(z_0 - z), z > z_0,$$

where k=1 kcal/mol - is the force constant, and z_0 is the position of the repulsive potential.

The distance to the repulsive potential of 60 A atop of C_5H_{11} groups ensures that the contact angle at the surface is not affected by perturbations in the CO_2 density caused by the wall.

Dynamics of the prepared quartz-C_5H_{11}-H_2O-CO_2 systems were simulated in NVT ensemble. Overall 1.5×10^6 production steps (3 ns simulation time) were performed for every system preceded by 3×10^5 equilibration steps. Duration of the production run for the surface with high alkyl surface density was chosen to provided sufficient time for the water droplet to detach from the surface and form a sphere floating in carbon dioxide. For the sake of fair comparison, simulations for the system with low alkyl

surface concentration were of the same length. Dimensions of the simulation boxes were 99.89x103.81x159.17 A. Figure S2 in the Supporting Information shows the initial simulation setups for two surfaces with pentyl surface densities of 1.45 and 2.89 C_5H_{12}/nm^2.

After the production runs an additional 5×10^4 simulation steps were performed at the same conditions. Five simulation snapshots separated by 10^4 steps were taken from these final runs for the analysis. The contact angle was calculated using the water iso-density charts constructed in coordinates height versus radius. Every data point of the iso-density chart represents a position in space where the water density is half of its normal density (0.033/2 water molecules per cubic angstrom). By varying the radius and the position of the centre, circles were fitted to the iso-density contours in such a way that a sum of absolute differences between the data points and the circle's profile is minimized, see Figure 5. The BFGS algorithm [61-64] was used for the minimization. The contact angle was next calculated as the angle of the tangential line to the circle's contour at its interception point with the surface. The surface was set at the tip level of pentyl groups which was found as the average position of the top three hydrogen atoms of all C_5H_{11} groups in the snapshot.

In contrast to an extremely hydrophilic fully hydroxylated quartz surface, the surface with a low concentration of surface pentyl groups (1.45 C_5H_{11}/nm^2) was found to be intermediate wet and the surface with a high concentration of surface pentyl groups (2.89 C_5H_{11}/nm^2) was found to be extremely hydrophobic. The contact angles at the tip level of pentyl groups are 118.6° (+/- 2.7°) and 180.0° for the surfaces with low and high pentyl surface density, respectively, see Figure 5; corresponding simulation snapshots are shown in Figure 6 and Figure 7. These results qualitatively agree with [5], where a calcite surface aged in a weak steric acid solution changed its wettability regime from hydrophilic (contact angle less than 90°) to hydrophobic (contact angle more than 90°) at 323 K and 10 MPa of CO_2 pressure.

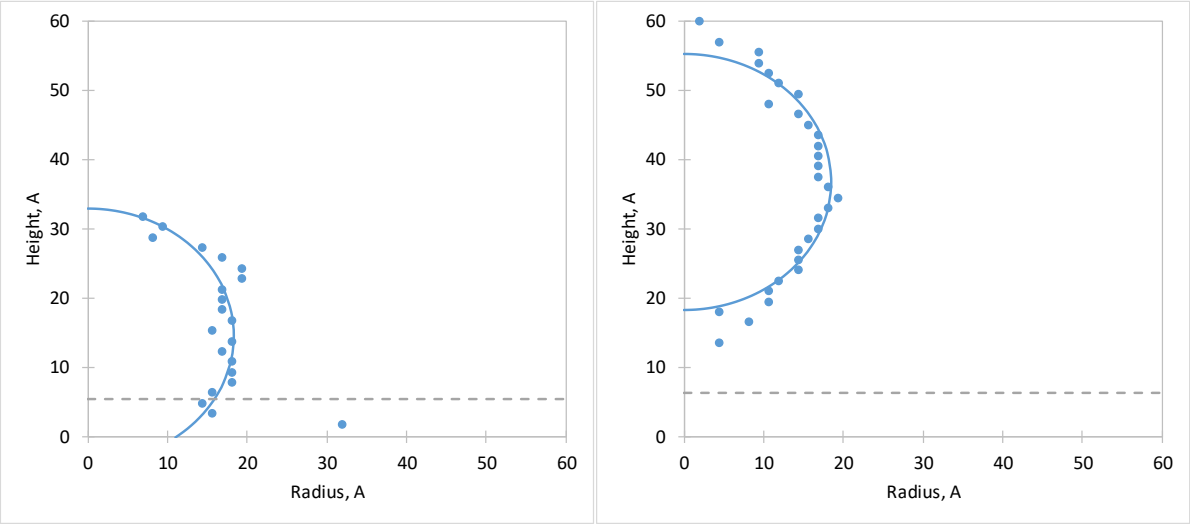

Figure 5. Circles fitted to the water iso-density for the hydroxylated quartz surfaces with a pentyl concentration of 1.45 (left) and 2.89 C_5H_{11}/nm^2 (right). Dashed line shows the tip level of pentyl groups.

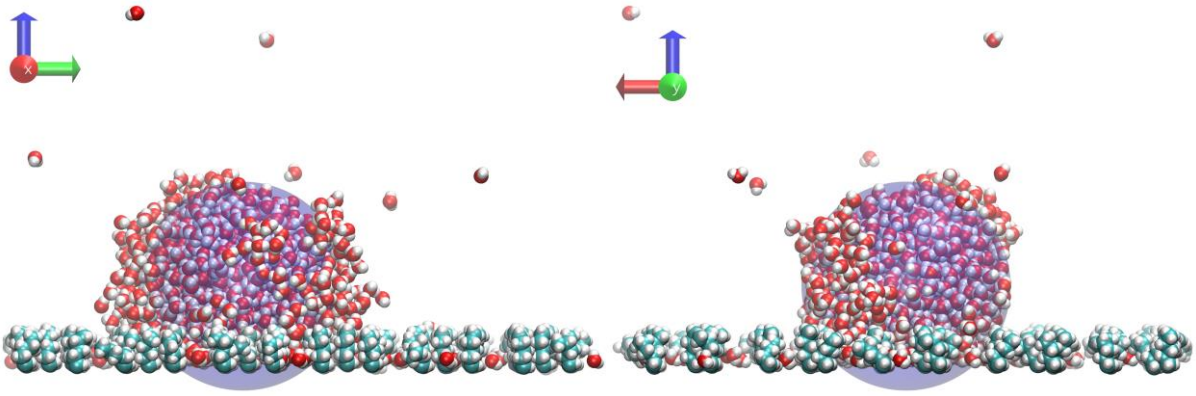

Figure 6. Simulation snapshot of the quartz surface with a pentyl concentration of 1.45 groups per square nm. View along x axis (left) and along y axis (right). The sphere fitted to the iso-density chart is illustrated in light purple color. Water molecules and pentyl groups are shown in VDW representation, white balls - hydrogen atoms, red balls - oxygen atoms, light blue balls - carbon atoms. Atoms of the CO_2 molecules and of the quartz slab are removed for clarity.

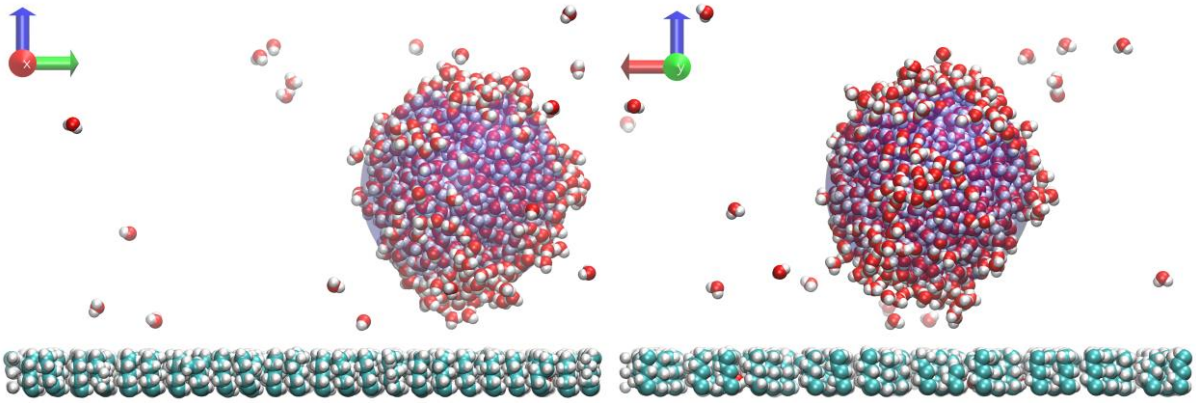

Figure 7. Simulation snapshot of the quartz surface with a pentyl concentration of 2.89 groups per square nm. View along x axis (left) and along y axis (right). The sphere fitted to the iso-density chart is illustrated in light purple color. Water molecules and pentyl groups are shown in VDW representation, white balls - hydrogen atoms, red balls - oxygen atoms, light blue balls - carbon atoms. Atoms of the CO_2 molecules and of the quartz slab are removed for clarity.

Interestingly, at a high pentyl surface density of 2.89 C_5H_{11}/nm^2, the water droplet loses contact with the surface and floats in the CO_2 phase. At this pentyl concentration the hydroxyl density is two times higher, 6.36 OH/nm^2. Note that similar hydroxyl concentration has been measured on real hydroxylated quartz surfaces under ambient conditions: 4.5-6.2 OH groups per nm^2 [65], 4.6-4.9 OH groups per nm^2 [66]. In contrast to these latter hydrophilic surfaces with almost the same OH density, the alkylated surface is completely hydrophobic. It is thus clear that pentyl groups, even at low concentration, have a dramatic effect on the contact angle.

Summary and Conclusions

To model quartz surfaces with chemisorpt hydrocarbons the CLAYFF [21] and DREIDING [24] force fields were coupled at atomic site charge level using the DFT and the Bader charge analysis. The charge of the hydroxyl hydrogen substituted with a pentyl group was reallocated to the newly formed oxygen-carbon bond connecting the C_5H_{11} group and quartz surface. Redistribution of the charge in proportion 0.796 to 0.204 for the carbon and the oxygen atoms, respectively, is shown to be consistent with the DFT results in terms of the absolute charge difference between the DFT charges and the force field charges on atoms of the OC bond, and in terms of the relative charges on both oxygen atoms of the

geminal silanol group. Our force field charges on the oxygen and the carbon atoms are computed to be -0.863301 and 0.338301 e.

Augmented with modified charges of the OC bond, the CLAYFF and the DREIDING force fields were applied to solve a practical problem of calculating the contact angle of a water droplet on alkylated quartz surfaces in a CO_2 environment. Alkylated quartz surfaces are shown to be hydrophobic despite their high surface concentration of hydroxyl groups. For pentyl surface density of 1.45 C_5H_{11}/nm^2 the contact angle at the tip level of pentyl groups was found to be 118.6°, and for the pentyl surface density of 2.89 C_5H_{11}/nm^2, the contact angle amounted to 180° (thus the water drop was floating in CO_2).

With the OC bond parameters obtained here, a systematic computational study of the influence of the surface density of chemisorpt hydrocarbons on the wettability of hydroxylated quartz is now possible and indeed technically required. In addition to this, taking into account a wide range of organic molecules sufficiently accurately modelled by the DREIDING force field, studies of quartz surfaces with chemisorpt via the OC bond species can also be performed with atomic site charges reported in this paper, not only in the context of surfaces' wettability.

Supporting Information

Parameters of the force fields, figures of alkylated quartz slab optimized at the DFT level of theory, figures of the initial simulation setups.

Acknowledgments

This work was supported by resources provided by the Pawsey Supercomputing Centre with funding from the Australian Government and the Government of Western Australia.

References

1. Bachu, S., Screening and ranking of sedimentary basins for sequestration of CO2 in geological media in response to climate change. *Environmental Geology* **2003,** *44* (3), 277-289.
2. IPCC *Carbon Dioxide Capture and Storage*; Intergovernmental Panel on Climate Change: 2005, 2005.
3. Arif, M.; Barifcani, A.; Lebedev, M.; Iglauer, S., Structural trapping capacity of oil-wet caprock as a function of pressure, temperature and salinity. *International Journal of Greenhouse Gas Control* **2016,** *50*, 112-120.
4. Iglauer, S.; Pentland, C. H.; Busch, A., CO2 wettability of seal and reservoir rocks and the implications for carbon geo-sequestration. *Water Resources Research* **2014,** *51* (1), 729-774.
5. Ali, M.; Al-Anssari, S.; Arif, M.; Barifcani, A.; Sarmadivaleh, M.; Stalker, L.; Lebedev, M.; Iglauer, S., Organic acid concentration thresholds for ageing of carbonate minerals: Implications for CO2 trapping/storage. *Journal of Colloid and Interface Science* **2019,** *534*, 88-94.
6. Giovambattista, N.; Debenedetti, P. G.; Rossky, P. J., Effect of Surface Polarity on Water Contact Angle and Interfacial Hydration Structure. *The Journal of Physical Chemistry B* **2007,** *111* (32), 9581-9587.
7. Bagherzadeh, S. A.; Englezos, P.; Alavi, S.; Ripmeester, J. A., Influence of Hydrated Silica Surfaces on Interfacial Water in the Presence of Clathrate Hydrate Forming Gases. *The Journal of Physical Chemistry C* **2012,** *116* (47), 24907-24915.
8. Iglauer, S.; Mathew, M. S.; Bresme, F., Molecular dynamics computations of brine–CO2 interfacial tensions and brine–CO2–quartz contact angles and their effects on structural and residual trapping mechanisms in carbon geo-sequestration. *Journal of Colloid and Interface Science* **2012,** *386* (1), 405-414.
9. McCaughan, J.; Iglauer, S.; Bresme, F., Molecular Dynamics Simulation of Water/CO2-quartz Interfacial Properties: Application to Subsurface Gas Injection. *Energy Procedia* **2013,** *37*, 5387-5402.

10. Chen, C.; Wan, J.; Li, W.; Song, Y., Water contact angles on quartz surfaces under supercritical CO2 sequestration conditions: Experimental and molecular dynamics simulation studies. *International Journal of Greenhouse Gas Control* **2015,** *42*, 655-665.
11. Liu, S.; Yang, X.; Qin, Y., Molecular dynamics simulation of wetting behavior at CO2/water/solid interfaces. *Chinese Science Bulletin* **2010,** *55* (21), 2252-2257.
12. Chen, C.; Zhang, N.; Li, W.; Song, Y., Water Contact Angle Dependence with Hydroxyl Functional Groups on Silica Surfaces under CO2 Sequestration Conditions. *Environmental Science & Technology* **2015,** *49* (24), 14680-14687.
13. Chen, C.; Chai, Z.; Shen, W.; Li, W.; Song, Y., Wettability of Supercritical CO2–Brine–Mineral: The Effects of Ion Type and Salinity. *Energy & Fuels* **2017,** *31* (7), 7317-7324.
14. Chen, C.; Chai, Z.; Shen, W.; Li, W., Effects of Impurities on CO2 Sequestration in Saline Aquifers: Perspective of Interfacial Tension and Wettability. *Industrial & Engineering Chemistry Research* **2018,** *57* (1), 371-379.
15. Tenney, C. M.; Cygan, R. T., Molecular Simulation of Carbon Dioxide, Brine, and Clay Mineral Interactions and Determination of Contact Angles. *Environmental Science & Technology* **2014,** *48* (3), 2035-2042.
16. Tsuji, S.; Liang, Y.; Kunieda, M.; Takahashi, S.; Matsuoka, T., Molecular Dynamics Simulations of the CO2-Water-silica Interfacial Systems. *Energy Procedia* **2013,** *37*, 5435-5442.
17. Liang, Y.; Tsuji, S.; Jia, J.; Tsuji, T.; Matsuoka, T., Modeling CO2–Water–Mineral Wettability and Mineralization for Carbon Geosequestration. *Accounts of Chemical Research* **2017,** *50* (7), 1530-1540.
18. Javanbakht, G.; Sedghi, M.; Welch, W.; Goual, L., Molecular Dynamics Simulations of CO2/Water/Quartz Interfacial Properties: Impact of CO2 Dissolution in Water. *Langmuir* **2015,** *31* (21), 5812-5819.
19. van Beest, B. W. H.; Kramer, G. J.; van Santen, R. A., Force fields for silicas and aluminophosphates based on ab initio calculations. *Physical Review Letters* **1990,** *64* (16), 1955-1958.
20. Emami, F. S.; Puddu, V.; Berry, R. J.; Varshney, V.; Patwardhan, S. V.; Perry, C. C.; Heinz, H., Force Field and a Surface Model Database for Silica to Simulate Interfacial Properties in Atomic Resolution. *Chemistry of Materials* **2014,** *26* (8), 2647-2658.
21. Cygan, R. T.; Liang, J.-J.; Kalinichev, A. G., Molecular Models of Hydroxide, Oxyhydroxide, and Clay Phases and the Development of a General Force Field. *The Journal of Physical Chemistry B* **2004,** *108* (4), 1255-1266.
22. Allinger, N. L.; Yuh, Y. H.; Lii, J. H., Molecular mechanics. The MM3 force field for hydrocarbons. 1. *Journal of the American Chemical Society* **1989,** *111* (23), 8551-8566.
23. Allinger, N. L.; Chen, K.; Lii, J.-H., An improved force field (MM4) for saturated hydrocarbons. *Journal of Computational Chemistry* **1996,** *17* (5-6), 642-668.
24. Mayo, S. L.; Olafson, B. D.; Goddard, W. A., DREIDING: a generic force field for molecular simulations. *The Journal of Physical Chemistry* **1990,** *94* (26), 8897-8909.
25. Lorentz, H. A., Ueber die Anwendung des Satzes vom Virial in der kinetischen Theorie der Gase. *Annalen der Physik* **1881,** *248* (1), 127-136.
26. Berthelot, D., Sur le mélange des gaz. *Comptes rendus hebdomadaires des séances de l'Académie des Sciences* **1898,** *126*, 1703-1855.
27. Anderson, R. S.; Anderson, S. P., *Geomorphology: The Mechanics and Chemistry of Landscapes*. Cambridge University Press: 2010.
28. Marshall, C. P.; Fairbridge, R. W., *Encyclopedia of Geochemistry*. Springer: 1999.
29. Allen, M. P.; Tildesley, D. J., *Computer Simulation of Liquids*. Clarendon Press: 1987; p 385.
30. Leach, A. R., *Molecular Modelling: Principles and Applications*. 2001; p 768.
31. Bleiziffer, P.; Schaller, K.; Riniker, S., Machine Learning of Partial Charges Derived from High-Quality Quantum-Mechanical Calculations. *Journal of Chemical Information and Modeling* **2018,** *58* (3), 579-590.

32. Cerutti, D. S.; Rice, J. E.; Swope, W. C.; Case, D. A., Derivation of Fixed Partial Charges for Amino Acids Accommodating a Specific Water Model and Implicit Polarization. *The journal of physical chemistry. B* **2013,** *117* (8), 2328-2338.
33. Giannozzi, P.; Baroni, S.; Bonini, N.; Calandra, M.; Car, R.; Cavazzoni, C.; Ceresoli, D.; Chiarotti Guido, L.; Cococcioni, M.; Dabo, I.; Corso Andrea, D.; Gironcoli Stefano, d.; Fabris, S.; Fratesi, G.; Gebauer, R.; Gerstmann, U.; Gougoussis, C.; Kokalj, A.; Lazzeri, M.; Martin-Samos, L.; Marzari, N.; Mauri, F.; Mazzarello, R.; Paolini, S.; Pasquarello, A.; Paulatto, L.; Sbraccia, C.; Scandolo, S.; Sclauzero, G.; Seitsonen Ari, P.; Smogunov, A.; Umari, P.; Wentzcovitch Renata, M., QUANTUM ESPRESSO: a modular and open-source software project for quantum simulations of materials. *Journal of Physics: Condensed Matter* **2009,** *21* (39), 395502.
34. Giannozzi, P.; Andreussi, O.; Brumme, T.; Bunau, O.; Nardelli, M. B.; Calandra, M.; Car, R.; Cavazzoni, C.; Ceresoli, D.; Cococcioni, M.; Colonna, N.; Carnimeo, I.; Corso, A. D.; Gironcoli, S. d.; Delugas, P.; R. A. DiStasio, J.; Ferretti, A.; Floris, A.; Fratesi, G.; Fugallo, G.; Gebauer, R.; Gerstmann, U.; Giustino, F.; Gorni, T.; Jia, J.; Kawamura, M.; Ko, H. Y.; Kokalj, A.; Küçükbenli, E.; Lazzeri, M.; Marsili, M.; Marzari, N.; Mauri, F.; Nguyen, N. L.; Nguyen, H. V.; Otero-de-la-Roza, A.; Paulatto, L.; Poncé, S.; Rocca, D.; Sabatini, R.; Santra, B.; Schlipf, M.; Seitsonen, A. P.; Smogunov, A.; Timrov, I.; Thonhauser, T.; Umari, P.; Vast, N.; Wu, X.; Baroni, S., Advanced capabilities for materials modelling with Q uantum ESPRESSO. *Journal of Physics: Condensed Matter* **2017,** *29* (46), 465901.
35. Bader, R. F. W., *Atoms in Molecules: A Quantum Theory*. Oxford University Press: 1994; p 456.
36. Henkelman, G.; Arnaldsson, A.; Jónsson, H., A fast and robust algorithm for Bader decomposition of charge density. *Computational Materials Science* **2006,** *36* (3), 354-360.
37. Sanville, E.; Kenny, S. D.; Smith, R.; Henkelman, G., Improved grid-based algorithm for Bader charge allocation. *Journal of Computational Chemistry* **2007,** *28* (5), 899-908.
38. Tang, W.; Sanville, E.; Henkelman, G., A grid-based Bader analysis algorithm without lattice bias. *Journal of Physics: Condensed Matter* **2009,** *21* (8), 084204.
39. Yu, M.; Trinkle, D. R., Accurate and efficient algorithm for Bader charge integration. *The Journal of Chemical Physics* **2011,** *134* (6), 064111.
40. Todorov, I. T.; Smith, W.; Trachenko, K.; Dove, M. T., DL_POLY_3: new dimensions in molecular dynamics simulations via massive parallelism. *Journal of Materials Chemistry* **2006,** *16* (20), 1911-1918.
41. Bush, I. J.; Todorov, I. T.; Smith, W., A DAFT DL_POLY distributed memory adaptation of the Smoothed Particle Mesh Ewald method. *Computer Physics Communications* **2006,** *175* (5), 323-329.
42. Humphrey, W.; Dalke, A.; Schulten, K., VMD: Visual molecular dynamics. *Journal of Molecular Graphics* **1996,** *14* (1), 33-38.
43. Momma, K.; Izumi, F., VESTA: a three-dimensional visualization system for electronic and structural analysis. *Journal of Applied Crystallography* **2008,** *41* (3), 653-658.
44. Swope, W. C.; Andersen, H. C.; Berens, P. H.; Wilson, K. R., A computer simulation method for the calculation of equilibrium constants for the formation of physical clusters of molecules: Application to small water clusters. *The Journal of Chemical Physics* **1982,** *76* (1), 637-649.
45. Hoover, W. G., Canonical dynamics: Equilibrium phase-space distributions. *Physical Review A* **1985,** *31* (3), 1695-1697.
46. Nosé, S., A molecular dynamics method for simulations in the canonical ensemble. *Molecular Physics* **1984,** *52* (2), 255-268.
47. Essmann, U.; Perera, L.; Berkowitz, M. L.; Darden, T.; Lee, H.; Pedersen, L. G., A smooth particle mesh Ewald method. *The Journal of Chemical Physics* **1995,** *103* (19), 8577-8593.
48. Darden, T.; York, D.; Pedersen, L., Particle mesh Ewald: An N·log(N) method for Ewald sums in large systems. *The Journal of Chemical Physics* **1993,** *98* (12), 10089-10092.
49. Berendsen, H. J. C.; Postma, J. P. M.; van Gunsteren, W. F.; Hermans, J., Interaction Models for Water in Relation to Protein Hydration. In *Intermolecular Forces: Proceedings of the Fourteenth Jerusalem Symposium on Quantum Chemistry and Biochemistry Held in Jerusalem, Israel, April 13–16, 1981*, Pullman, B., Ed. Springer Netherlands: Dordrecht, 1981; pp 331-342.

50. Harris, J. G.; Yung, K. H., Carbon Dioxide's Liquid-Vapor Coexistence Curve And Critical Properties as Predicted by a Simple Molecular Model. *The Journal of Physical Chemistry* **1995,** *99* (31), 12021-12024.
51. Perdew, J. P.; Burke, K.; Ernzerhof, M., Generalized Gradient Approximation Made Simple. *Physical Review Letters* **1996,** *77* (18), 3865-3868.
52. Goumans, T. P. M.; Wander, A.; Brown, W. A.; Catlow, C. R. A., Structure and stability of the (001) α-quartz surface. *Physical Chemistry Chemical Physics* **2007,** *9* (17), 2146-2152.
53. Murashov, V. V., Reconstruction of Pristine and Hydrolyzed Quartz Surfaces. *The Journal of Physical Chemistry B* **2005,** *109* (9), 4144-4151.
54. Yang, J.; Wang, E. G., Water adsorption on hydroxylated alpha-quartz (0001) surfaces: From monomer to flat bilayer. *Physical Review B* **2006,** *73* (3), 035406.
55. Adeagbo, W. A.; Doltsinis, N. L.; Klevakina, K.; Renner, J., Transport Processes at α-Quartz–Water Interfaces: Insights from First-Principles Molecular Dynamics Simulations. *ChemPhysChem* **2008,** *9* (7), 994-1002.
56. Monkhorst, H. J.; Pack, J. D., Special points for Brillouin-zone integrations. *Physical Review B* **1976,** *13* (12), 5188-5192.
57. Blöchl, P. E., Projector augmented-wave method. *Physical Review B* **1994,** *50* (24), 17953-17979.
58. www.quantum-espresso.org Quantum ESPRESSO. www.quantum-espresso.org.
59. Levien, L.; Prewitt, C. T.; Weidner, D. J., Structure and elastic properties of quartz at pressure. *American Mineralogist* **1980,** *65* (9-10), 920-930.
60. webbook.nist.gov NIST Chemistry WebBook. https://webbook.nist.gov/chemistry/.
61. Broyden, C. G., The Convergence of a Class of Double-rank Minimization Algorithms 1. General Considerations. *IMA Journal of Applied Mathematics* **1970,** *6* (1), 76-90.
62. Fletcher, R., A new approach to variable metric algorithms. *The Computer Journal* **1970,** *13* (3), 317-322.
63. Goldfarb, D., A Family of Variable-Metric Methods Derived by Variational Means. *Mathematics of Computation* **1970,** *24* (109), 23-26.
64. Shanno, D. F., Conditioning of Quasi-Newton Methods for Function Minimization. *Mathematics of Computation* **1970,** *24* (111), 647-656.
65. Iler, R. K., *The Chemistry of Silica: Solubility, Polymerization, Colloid and Surface Properties and Biochemistry of Silica*. John Wiley & Sons (Wiley-Interscience Publication): 1979; p 896.
66. Zhuravlev, L. T., The surface chemistry of amorphous silica. Zhuravlev model. *Colloids and Surfaces A: Physicochemical and Engineering Aspects* **2000,** *173* (1), 1-38.

TOC Graphic (For Table of Contents Use Only)

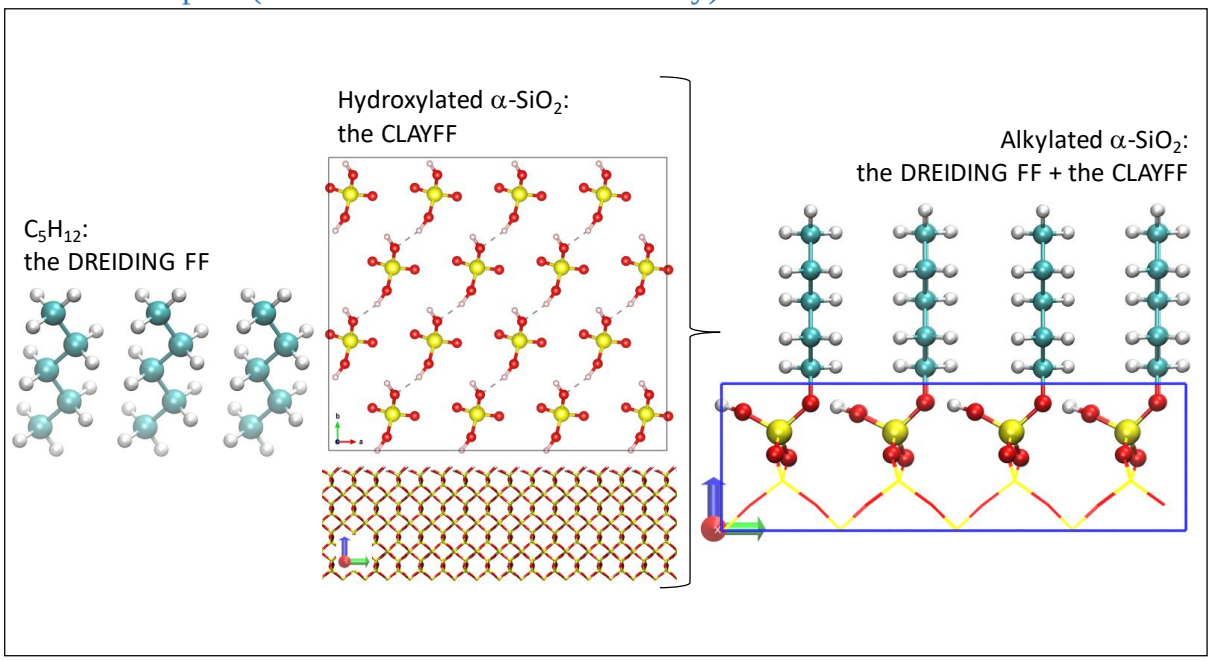

Application of the CLAYFF and the DREIDING Force Fields for Modelling of Alkylated Quartz Surfaces

Aleksandr Abramov, Stefan Iglauer, School of Engineering, Edith Cowan University, 270 Joondalup Drive, Joondalup, WA 6027, Western Australia, Australia

aabramov@our.ecu.edu.au

Force Fields

In all simulations water and carbon dioxide molecules were treated as rigid bodies. In the initial preparation of the hydroxylated quartz surface the OH groups were also modelled as rigid bodies. Geometries of the rigid bodies were reproduced according to corresponding molecular models and force fields: CO distance (EPM2 CO_2) 1.149 A; OH distance (SPC H_2O) 1 A; HOH angle (SPC H_2O) 109.47°; OH distance (hydroxyl) 1 A. To get convenient for pentyl groups integration onto the surface orientation of the OH groups involved in the weak hydrogen bonds (pointing slightly upwards, see [1-2]), and to highlight and isolate the weak hydrogen bonds - the place of attachment of the pentyl groups, only non-bond CLAYFF force field terms were used in the initial preparation of the hydroxylated quartz surface. All OH bond and Si-O-H angular potentials of the silanol groups were accounted for in the equilibration and the production runs of the fully assembled systems (alkylated quartz surface, water droplet, molecules of the CO_2 phase).

Parameters of potentials used to model the van der Waals interactions between all atomic species of studied in this work systems are listed in Table S1.

Table S1. Non-bond potential parameters used in the simulations [3-4].

Atomic species	A, A^{12}·kcal/mol	B, A^{6}·kcal/mol	q, e	m, amu
C (CO_2)	4.31282×10^4	9.82063×10^1	0.6512	12.0107
O (CO_2)	3.87857×10^5	4.98236×10^2	-0.3256	15.9994
O (H_2O)	6.29342×10^5	6.25459×10^2	-0.82	15.9994
H (H_2O)	0	0	0.41	1.0079
Si (SiO_2))	1.23698×10^1	9.54288×10^{-3}	2.1	28.0855
O (SiO_2 bridging)	6.293422×10^5	6.254591×10^2	-1.05	15.9994
O (SiO_2 hydroxyl)	6.293422×10^5	6.254591×10^2	-0.95	15.9994
H (SiO_2 hydroxyl)	0	0	0.425	1.0079
C (O-C_5H_{11})	1171341.71	667.516584	0 (0.338301)*	12.0107
H (O-C_5H_{11})	17198.6333	32.3369279	0	1.0079
O (O-C_5H_{11})	232115.998	298.083888	-0.863301**	15.9994

*charge on carbon of the OC bond is shown in brackets (estimated on basis of DFT calculations); **estimated on basis of DFT calculations.

Parameters in Table S1 correspond to the following analytical expression for the non-bond potential (U):

$$U(r) = \frac{A}{r^{12}} - \frac{B}{r^{6}},$$

where r is the interatomic distance.

To convert original CLAYFF parameters (D_0, R_0) to parameters of provided representation of the 12-6 potential the following formulae were used:

$$A = D_0 R_0^{12},$$

$$B = 2D_0 R_0^6.$$

The EPM2 potential parameters were converted to parameters of the 12-6 potential using formulae:

$$A = 4\varepsilon\sigma^{12},$$

$$B = 4\varepsilon\sigma^6.$$

The interaction parameters between the unlike atoms were obtained as the geometric mean for both A and B:

$$A_{ij} = \sqrt{A_i A_j},$$

$$B_{ij} = \sqrt{B_i B_j},$$

where i and j are indices of the unlike atoms.

In fully assembled systems, apart from the rigid bodies (water and carbon dioxide molecules), all bonds and angles were treated explicitly using bond and angle potentials. Energy of every bond stretch was described by a harmonic relationship:

$$U(r_{ij}) = \frac{k_1}{2}(r_{ij} - r_0)^2,$$

where k_1 is the force constant, and r_0 represents the equilibrium bond length, see Table S2.

Table S2. Bond stretch parameters used in the simulations [3-4].

Species i	Species j	k_1, kcal/mol/A^2	r_0, A
O (SiO_2 hydroxyl)	H (SiO_2 hydroxyl)	1108.2698	1.0
C (O-C_5H_{11})	H (O-C_5H_{11})	700.0	1.09
C (O-C_5H_{11})	C (O-C_5H_{11})	700.0	1.53
C (O-C_5H_{11})	O (O-C_5H_{11})	700.0	1.33
Si (SiO_2)	O (O-C_5H_{11})	700.0	1.497

The Si-O-H angles (θ) of attached to the quartz surface hydroxyl groups were restrained by the harmonic potential:

$$U(\theta) = \frac{k_2}{2}(\theta - \theta_0)^2,$$

where k_2 = 60.0 kcal/mol/rad^2 is the force constant, and θ_0 = 109.47° is the equilibrium bond angle [3].

Bending of the Si-O-C_5H_{11} angles of attached to the quartz surface O-C_5H_{11} groups were modelled and parametrized according to the harmonic cosine potential:

$$U(\theta) = \frac{k_3}{2}(\cos\theta - \cos\theta_0)^2,$$

where k_3 = 133.333333 kcal/mol is the force constant, and θ_0 = 120.0° is the equilibrium bond angle [4].

Bending of all intramolecular angles of the O-C_5H_{11} groups were modelled and parametrized using the harmonic cosine potential:

$$U(\theta) = \frac{k_4}{2}(\cos\theta - \cos\theta_0)^2,$$

where k_4 = 112.499693 kcal/mol is the force constant, and θ_0 = 109.471° is the equilibrium bond angle [4].

Torsion of all intramolecular dihedral angles (φ) of the O-C_5H_{11} groups were modelled and parametrized according to the cosine potential:

$$U(\varphi) = A_2(1 + \cos 3\varphi),$$

where A_2 = 0.11111111 kcal/mol [4].

Figures

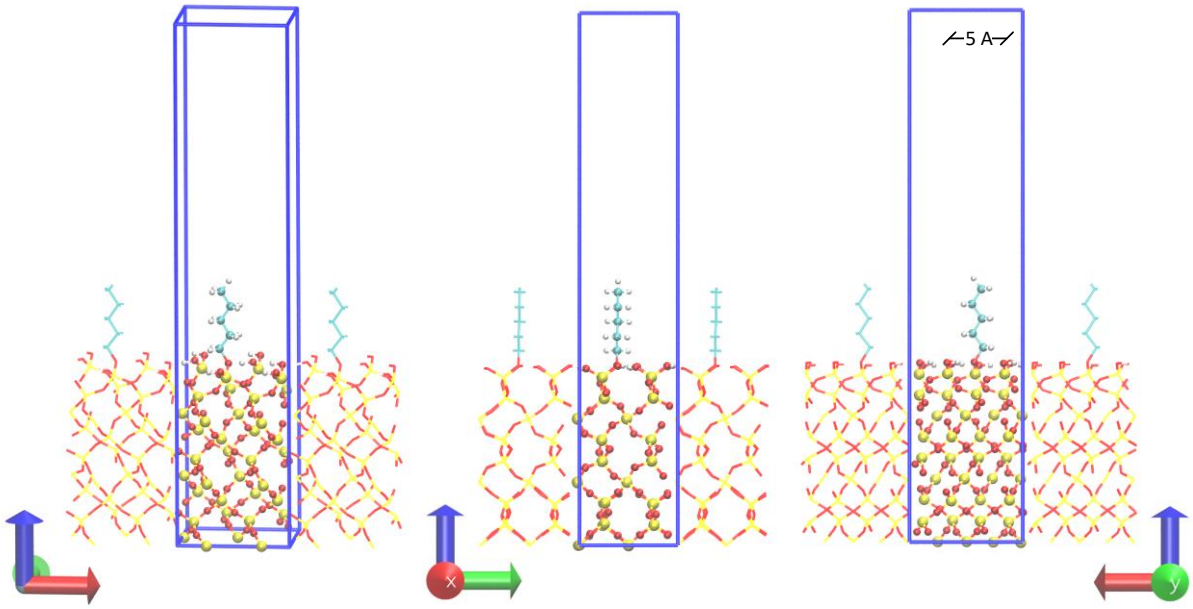

Figure S1. Optimized at the DFT level of theory quartz slab, side view and views along the x and y axis. White balls - hydrogen atoms, light blue balls - carbon atoms, red balls - oxygen atoms, yellow balls - silicon atoms. Blue lines demark the unit cell of the simulated system, images of the unit cell are shown with lines instead of the balls.

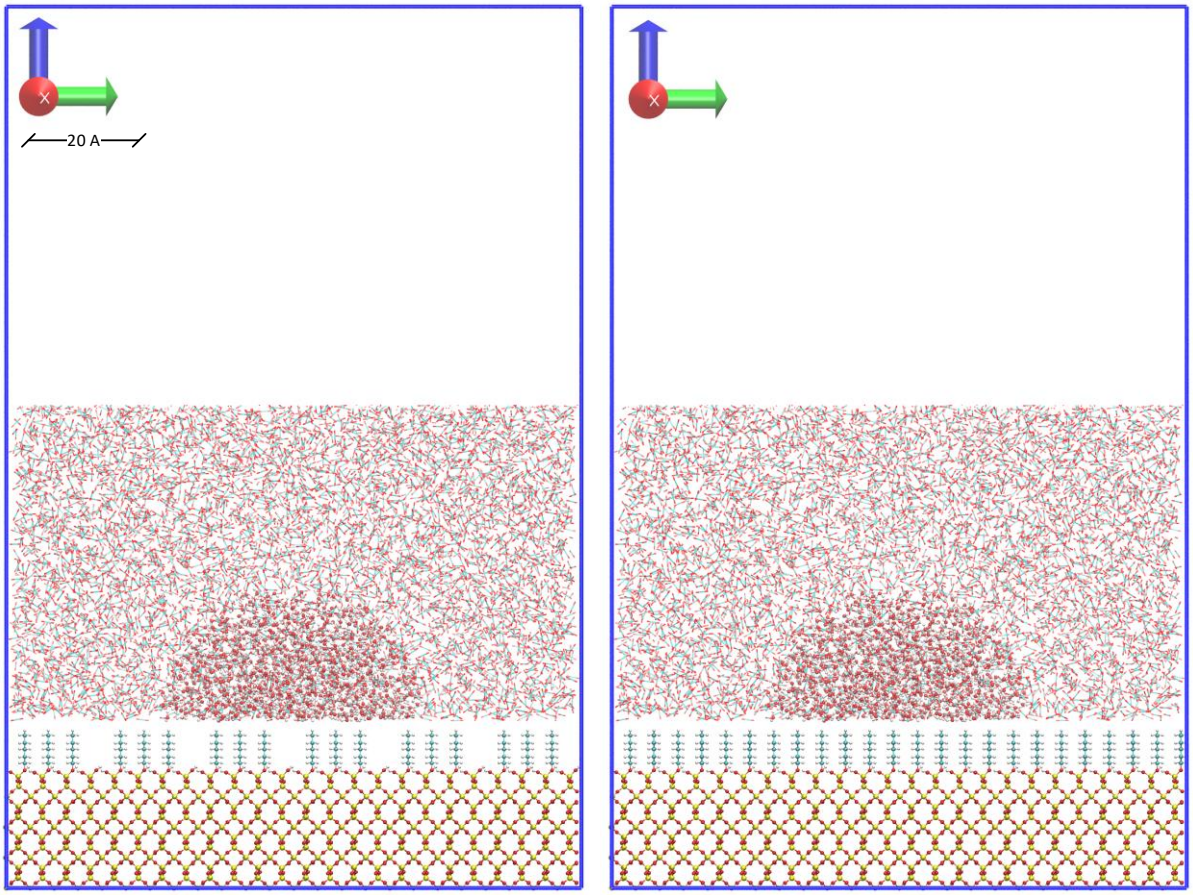

Figure S2. Side views of the initial simulation setups for quartz surfaces with C_5H_{11} density 1.45 (left) and 2.89 (right) groups per square nanometre. White balls - hydrogen atoms, red balls - oxygen atoms, light blue balls - carbon atoms, yellow balls - silicon atoms. CO_2 molecules are shown with lines to improve visibility of the water droplet.

References

1. Murashov, V. V., Reconstruction of Pristine and Hydrolyzed Quartz Surfaces. *The Journal of Physical Chemistry B* **2005,** *109* (9), 4144-4151.
2. Goumans, T. P. M.; Wander, A.; Brown, W. A.; Catlow, C. R. A., Structure and stability of the (001) α-quartz surface. *Physical Chemistry Chemical Physics* **2007,** *9* (17), 2146-2152.
3. Cygan, R. T.; Liang, J.-J.; Kalinichev, A. G., Molecular Models of Hydroxide, Oxyhydroxide, and Clay Phases and the Development of a General Force Field. *The Journal of Physical Chemistry B* **2004,** *108* (4), 1255-1266.
4. Mayo, S. L.; Olafson, B. D.; Goddard, W. A., DREIDING: a generic force field for molecular simulations. *The Journal of Physical Chemistry* **1990,** *94* (26), 8897-8909.